Transport Model of Optical Beams in a Plasma

T. Kurki-Suonio and T. Tajima
Department of Physics and Institute for Fusion Studies
The University of Texas at Austin
Austin, Texas 78712

August 1988

Transport Model of Optical Beams in a Plasma

T. Kurki-Suonio and T. Tajima
Department of Physics and Institute for Fusion Studies
The University of Texas at Austin
Austin, Texas 78712

Abstract

A new kind of a particle simulation algorithm suitable for following long time scale evolution of electromagnetic beams in plasma is presented. The algorithm is based on particle and field equations averaged over the rapid laser oscillations and the model constitutes the electromagnetic counterpart for the Zakharov's model for electrostatics. Computational remarks upon implementation of the algorithm are given. Test results of the code applied to the Rayleigh spread and self-focusing of an intense laser beam in a plasma are discussed.

I. Introduction

The simulation of the physical behavior of high frequency electromagnetic beams propagating in a plasma involves several aspects. First, in terms of frequency scales, the electromagnetic radiation has typically very high frequency (unless it is in resonance or propagates in an overdense plasma), $\omega_0 \sim ck_0$, where k_0 is the wavenumber of the wave and c is the speed of light. Secondly, plasma oscillations involve the electron plasma frequency $\omega_p = \sqrt{\frac{4\pi n e^2}{m}}$ which is typically much smaller than the photon frequency ω_0 in an underdense plasma. In what follows we concern ourselves primarily with underdense plasmas. Thirdly, there are time scales associated with ions (such as the ion plasma frequency ω_{pi}, and ion acoustic frequency $k_0 c_s$ with c_s being the sound speed) and those associated with the transport of the optical beam (including diffusion, diffraction, scattering and dissipation (depletion)). Some of these processes may involve plasma instabilities such as parametric instabilities.

Similar hierarchy of spatial scales can be discerned as well. They are the electromagnetic wavelength, plasma wavelength and the Debye length, the dimensions of the optical beam (the width and the length), and the transport length such as the depletion length.

The interrelation between the high frequency electromagnetic waves and the plasma oscillations has been an active area of research and the computational efforts have been fairly well documented.[1-3] However, the investigation of the beam dynamics over longer time scales and larger spatial extent is less developed. Some attempts have been made[4] but these tend to be not fully self-consistent. It is of vital importance, therefore, to develop a numerical model that encompasses over time scales much longer than the radiation time scale and that can follow the overall dynamics (i.e. transport) of the optical beam. Only with such a model one can fully study, for example, the long time scale evolution and transport of the beam in applications to the beat wave accelerator[1] and the plasma fiber accelerator.[5]

2

In these applications it is important to make the length of the optical beam sufficiently short so that it does not induce instabilities related to ionic responses. This simplifies the experimental situations along with the computational considerations. In what follows we confine ourselves to these circumstances only.

The present effort of model development may be regarded as an electromagnetic counterpart to the Zakharov model[6] of electrostatic pulses and to the subsequent numerical calculations.[7,8] In Sec. II we present our model of time-averaged (or phase-averaged) equations: the equations governing the evolution of the electromagnetic fields and the particle dynamics are averaged over the rapid laser oscillations. This way only the secular changes in field quantities will be followed. Also, since typically the amplitude of the modulation is much smaller than the amplitude of the wave, this scheme has the additional advantage of making the signal cleaner by averaging out the masking dominant oscillations. In Sec. III computational algorithmic considerations are discussed. Test results of the code (for Rayleigh spread in vacuum and self-focusing of an intense optical beam in a plasma) are discussed in Sec. IV, followed by the conclusions in final Sec. V.

II.   Mathematical Formulation

The basic idea in developing the mathematical model for computation is to average the equations evolving the electromagnetic field and electrons (the ions are assumed to be stationary in this first version) over the short laser oscillation period. That way we eliminate the fast time scale of the uninteresting rapid oscillations and follow only the slower time scales associated with the net changes in quantities of interest. The averaging in space and time can be carried out simultaneously provided the ansatz is chosen appropriately.

Consider the wave equation for the vector potential instead of the set of Maxwell's equations for the electric and magnetic fields. This is done because averaging Maxwell's equations over the laser oscillation period would lead to a set of trivial identities. Further, if we had

chosen to study the wave equation in terms of either electric or magnetic field, the plasma contribution would appear as the time derivative of the plasma current, whereas when using the vector potential the plasma current as such appears in the wave equation. Writing the electric and magnetic fields in terms of their potentials,

$$\mathbf{E} \equiv -\nabla\Phi - \frac{\left(\frac{1}{c}\right)\partial\mathbf{A}}{\partial t} \quad , \quad \mathbf{B} \equiv \nabla \times \mathbf{A} \,, \tag{1}$$

the wave equation, derived from Maxwell's equations, becomes

$$\left(\frac{1}{c^2}\right)\frac{\partial^2\mathbf{A}}{\partial t^2} - \nabla^2\mathbf{A} + \frac{\left(\frac{1}{c}\right)\nabla\partial\Phi}{\partial t} = \left(\frac{4\pi}{c}\right)\mathbf{J} \,. \tag{2}$$

The Coulomb's gauge, $\nabla \cdot \mathbf{A} = 0$, is chosen for the potentials. This allows a clear separation of slowly and rapidly varying quantities. For instance, in the case of the electric field, the rapidly varying electromagnetic part is entirely given by the vector potential. The scalar potential like the particle density, on the other hand, is slowly varying (the variations in particle density are slow compared to the laser oscillations because they are produced by the slow time scale ponderomotive force):

$$\nabla \cdot \mathbf{E} = 4\pi e(n_i - n_e) \Rightarrow \nabla^2\Phi = 4\pi e(n_i - n_e) \,. \tag{3}$$

For simplicity, the electromagnetic fields are assumed to have circular polarization and the vector potential is written in the form

$$\mathbf{A}(\mathbf{x}, t) = a(\mathbf{x}, t)\exp\left\{ik_0 z - i\omega_0 t - i\psi(\mathbf{x}, t)\right\}(\hat{x} + i\hat{y}) \,, \tag{4}$$

where amplitude 'a' and phase shift 'ψ' are slowly varying (compared to the laser oscillations), real quantities:

$$\begin{aligned} \frac{\partial\psi}{\partial t} &\ll \omega_0 & \frac{\partial\psi}{\partial z} &\ll k_0 \\ \frac{\partial a}{\partial t} &\ll \omega_0 a & \frac{\partial a}{\partial z} &\ll k_0 a \,. \end{aligned} \tag{5}$$

4

The averaging over laser oscillations now becomes straightforward for most terms in the wave equation:

$$\frac{1}{T_0} \int |\mathbf{A}|^2 dt = \frac{1}{2} \mathbf{A} \cdot \mathbf{A}^* = a(\mathbf{x}, t)^2$$
$$\frac{1}{\lambda_0} \int |\mathbf{A}|^2 dz = \frac{1}{2} \mathbf{A} \cdot \mathbf{A}^* = a(\mathbf{x}, t)^2 \ . \tag{6}$$

Using the expression (4) for the vector potential and multiplying the wave equation by the complex conjugate of $\mathbf{A}$, the real part of the wave equation yields an averaged partial differential equation for the amplitude, $a(\mathbf{x}, t)$, and the imaginary part an averaged equation for the phase shift, $\psi(\mathbf{x}, t)$:

$$\frac{\partial^2}{\partial t^2} a = c^2 \nabla^2 a + a \left[\left(\frac{\partial \psi}{\partial t} \right)^2 - c^2 |\nabla \psi|^2 \right] + 2a \left[\omega_0 \frac{\partial \psi}{\partial t} + c k_0 \frac{\partial \psi}{\partial z} \right] + \left(\frac{4\pi}{c} \right) \mathrm{Re}(\mathbf{J} \cdot \mathbf{A}^*) \tag{7}$$

and

$$\frac{\partial}{\partial t} \left(a^2 \frac{\partial \psi}{\partial t} \right) = c^2 \nabla \cdot (a^2 \nabla \psi) - 2a \left(\omega_0 \frac{\partial a}{\partial t} + c k_0 \frac{\partial a}{\partial z} \right) - \left(\frac{4\pi}{c} \right) \mathrm{Im}(\mathbf{J} \cdot \mathbf{A}^*) \ . \tag{8}$$

In deriving an expression for the plasma current we assume that the ions, being much heavier than the electrons, can be regarded stationary over the period of interest. This is motivated by our desire to operate in a regime void of parametric instabilities (see Barnes et al.[9]). Thus the current can be written in the form:

$$\mathbf{J} \approx \sum_\alpha q_\alpha n_\alpha \mathbf{v}_\alpha \approx -e n_e \mathbf{v}_e \ . \tag{9}$$

The electron contribution to the plasma current is obtained by using the relativistic equation of motion:

$$n_e \frac{\partial}{\partial t} \mathbf{p} + n_e \mathbf{v} \cdot \nabla \mathbf{p} = -e n_e \mathbf{E} - \left(\frac{e n_e}{c} \right) \mathbf{v} \times \mathbf{B} - \nabla P \ ,$$

$$\mathbf{p} = m \gamma \mathbf{v} \quad , \quad \gamma = \sqrt{1 + \frac{p^2}{m^2 c^2}} \ , \tag{10}$$

where P is the pressure of the electron fluid. (The subscript 'e' has now been dropped from the electron velocity). We will expand the electron velocity (as well as momentum) in terms

5

of the normalized quivering velocity $\mu \equiv \frac{ea}{mc^2} < 1$. In order to include the ponderomotive effects it is necessary to keep terms up to the second order in μ. To incorporate the effects due to the electron density depression we need to keep terms up to the third order in μ. Keeping terms up to the third order only, we can drop the pressure term, because it is of the fourth order in μ:

$$\nabla P \sim T_e \nabla \delta n_e \sim v_{\text{th}}^2 \nabla \delta n_e \sim \left(\frac{v_{\text{th}}}{v_{\text{osc}}} \right)^2 \mu^2 \nabla \delta n_e , \tag{11}$$

and, as recalled from the previous chapter, δn_e is of the order of μ^2, and so

$$\nabla P \sim \left(\frac{v_{\text{th}}}{v_{\text{osc}}} \right)^2 O(\mu^4) .$$

The equation of motion for electrons, therefore, can be written as

$$\frac{\partial}{\partial t} (\mathbf{p}_1 + \mathbf{p}_2 + \mathbf{p}_3) + \mathbf{v}_1 \cdot \nabla(\mathbf{p}_1 + \mathbf{p}_2) + \mathbf{v}_2 \cdot \nabla \mathbf{p}_1$$

$$= e\nabla\Phi + \left(\frac{e}{c} \right) \frac{\partial \mathbf{A}}{\partial t} + \left(\frac{e}{c} \right) (\mathbf{v}_1 + \mathbf{v}_2) \times (\nabla \times \mathbf{A}) , \tag{12}$$

and the plasma current as

$$\mathbf{J} \approx -en_0(\mathbf{v}_1 + \mathbf{v}_2 + \mathbf{v}_3) - e\delta n_e \mathbf{v}_1 . \tag{13}$$

It is important to notice that even though the thermal velocity of the electrons does not contribute to the plasma current explicitly, it still affects the current through the relativistic mass increase of the electrons:

$$\gamma = \sqrt{1 + \frac{(\mathbf{p}_0 + \mathbf{p}_1 + \mathbf{p}_2 + \mathbf{p}_3)^2}{m^2 c^2}} , \tag{14}$$

where $\mathbf{p}_0$ denotes the momentum corresponding to the thermal velocity. In case of a cool plasma the effect of p_0 is, of course, negligible.

The electron momenta in different orders, as obtained from the relativistic equation of motion, are given by:

$$\mathbf{p}_1 = \left(\frac{e}{c}\right)\mathbf{A} ,$$

$$\frac{\partial}{\partial t}\mathbf{p}_2 = e\nabla\Phi - \left(\frac{e}{c}\right)\mathbf{v}_1 \times (\nabla \times \mathbf{A}) ,$$

$$\frac{\partial}{\partial t}\mathbf{p}_3 = \mathbf{v}_1 \cdot \nabla\mathbf{p}_2 + \mathbf{v}_2 \cdot \nabla\mathbf{p}_1 - \left(\frac{e}{c}\right)\mathbf{v}_2 \times (\nabla \times \mathbf{A}) . \tag{15}$$

In order to express the momenta in terms of the field quantities only, we need to define the different order velocities v_i, $i = 1, 2, 3$. This may be done by expanding the relativistic gamma in powers of μ:

$$\frac{1}{\gamma} = \frac{1}{\sqrt{1 + \frac{p^2}{m^2 c^2}}} \approx \left(\frac{1}{\gamma_0}\right)\left\{1 - \left(\frac{1}{m^2 c^2 \gamma_0^2}\right)\left[\mathbf{p}_0 \cdot \mathbf{p}_1 + \frac{1}{2}p_1^2 + \mathbf{p}_0 \cdot \mathbf{p}_2\right.\right.$$

$$\left.\left. + \mathbf{p}_0 \cdot \mathbf{p}_3 + \mathbf{p}_1 \cdot \mathbf{p}_2\right]\right\} , \tag{16}$$

where $\gamma_0 \equiv \sqrt{1 + \frac{p_0^2}{m^2 c^2}}$. Using this expression for the electron velocities in different orders they become:

$$\mathbf{v}_1 = \left(\frac{\mathbf{p}_1}{m\gamma_0}\right)$$

$$\mathbf{v}_2 = \left(\frac{\mathbf{p}_2}{m\gamma_0}\right)$$

$$\mathbf{v}_3 = \left(\frac{1}{m\gamma_0}\right)\left[\mathbf{p}_3 - \frac{1}{2}\left(\frac{1}{m\gamma_0}\right)^2 p_1^2\mathbf{p}_1\right] , \tag{17}$$

where we noted that the terms with odd powers of the thermal velocity vanish. Using these expressions for the electron velocity, we can now write all the different order electron momenta in terms of the field quantities:

$$\mathbf{p}_1 = \left(\frac{e}{c}\right)\mathbf{A} ,$$

$$\frac{\partial}{\partial t}\mathbf{p}_2 = e\nabla\Phi - \left(\frac{e^2}{2m\gamma_0 c^2}\right)\nabla a^2 \qquad \text{and} \qquad (18)$$

$$\frac{\partial}{\partial t}\mathbf{p}_3 = -\left(\frac{e}{m\gamma_0 c}\right)[\mathbf{A}\cdot\nabla\mathbf{p}_2 + (\nabla\mathbf{A})\cdot\mathbf{p}_2] .$$

The expression for the second order momenta consists of only slowly varying terms (Φ and a) and it will be kept in the differential form: In the code we will store $\mathbf{p}_2$ as a grid quantity and advance it explicitly. The third order momenta, however, consists of both slowly and rapidly varying terms, and we find an expression for $\mathbf{p}_3$ by approximating the behavior of rapidly varying terms by $\exp(-i\omega_0 t)$:

$$\mathbf{p}_3 \approx -i\left(\frac{e}{m\gamma_0 c\omega_0}\right)[\mathbf{A}\cdot\nabla\mathbf{p}_2 + (\nabla\mathbf{A})\cdot\mathbf{p}_2] . \qquad (19)$$

The different order electron velocities are now given by

$$\mathbf{v}_1 = \left(\frac{e}{m\gamma_0 c}\right)\mathbf{A}$$

$$\mathbf{v}_2 = \left(\frac{1}{m\gamma_0}\right)\mathbf{p}_2 \qquad (20)$$

$$\mathbf{v}_3 = -\left(\frac{e}{m^2\gamma_0^2 c}\right)\left\{\frac{1}{2}\left(\frac{e^2}{2m\gamma_0 c^4}\right)a^2\mathbf{A} + \left(\frac{i}{\omega_0}\right)[\mathbf{A}\cdot\nabla\mathbf{p}_2 + (\nabla\mathbf{A})\cdot\mathbf{p}_2]\right\} .$$

Having everything in the plasma current expressed in terms of the field potentials, we can carry out the averaging over the rapid laser oscillations. As in the case of the left hand side of the wave equation, this is done by multiplying the plasma current by the complex conjugate of the vector potential and averaging over the laser oscillation period. The first order current is

$$\mathbf{J}_1 = -en_0\mathbf{v}_1 \qquad \text{and so}$$

$$\left(\frac{1}{T_0}\right)\int\mathbf{J}_1\cdot\mathbf{A}^* dt = -2\left(\frac{e^2 n_0}{m\gamma_0 c}\right)a^2 . \qquad (21)$$

The second order current is slowly varying and therefore it vanishes upon averaging. The third order current calls for special care. It contains terms that are not proportional to

8

the vector potential. Therefore, if we multiply it by the complex conjugate of the vector potential, unphysical terms will arise due to phase mixing. To avoid this, the term not proportional to **A** must be averaged using real representation. The third order current is given by

$$\mathbf{J}_3 = -e(n_0\mathbf{v}_3 + \delta n_e\mathbf{v}_1) = -\left(\frac{en_0}{m\gamma_0}\right)\left[\mathbf{p}_3 - \frac{1}{2}(mc\gamma_0)^2\, p_1^2\mathbf{p}_1\right] - e\delta n_e\mathbf{v}_1\;. \tag{22}$$

The two latter terms, being proportional to **A** can be averaged using complex notation:

$$\begin{aligned}\left(\frac{1}{T_0}\right)\int \delta n_e\mathbf{v}_1\cdot\mathbf{A}^*dt &\approx 2\left(\frac{e\delta n_e}{mc\gamma_0}\right)a^2\;,\\\left(\frac{1}{T_0}\right)\int \delta n_e\mathbf{v}_1\cdot\mathbf{A}^*dt &\approx 2\left(\frac{e}{c}\right)^3 a^4\;.\end{aligned} \tag{23}$$

Averaging the first term in the expression for $\mathbf{J}_3$ we return to real notation:

$$\mathbf{p}_3 = -i\left(\frac{e}{mc\gamma_0\omega_0}\right)\left[\mathbf{A}\cdot\boldsymbol{\nabla}\mathbf{p}_2 + (\boldsymbol{\nabla}\mathbf{A})\cdot\mathbf{p}_2\right]\;. \tag{24}$$

Carrying out the averaging term by term, we find

$$\begin{aligned}\left(\frac{1}{T_0}\right)\int \mathbf{A}\cdot[\mathbf{A}\cdot\boldsymbol{\nabla}\mathbf{p}_2]dt &= \left(\frac{1}{T_0}\right)\int A_jA_i\partial_ip_{2_j}dt \approx \partial_ip_{2_j}\left(\frac{1}{T_0}\right)\int A_iA_jdt\\&= \partial_ip_{2_j}\left(\frac{1}{2}a^2\delta_{i,j}\right)\qquad\text{for}\qquad i,j=x,y\\&= \frac{1}{2}a^2\boldsymbol{\nabla}_T\cdot\mathbf{p}_2\;,\end{aligned} \tag{25}$$

where $\boldsymbol{\nabla}_T \equiv \hat{x}\frac{\partial}{\partial x} + \hat{y}\frac{\partial}{\partial y}$, and

$$\begin{aligned}\left(\frac{1}{T_0}\right)\int \mathbf{A}\cdot[(\boldsymbol{\nabla}\mathbf{A})\cdot\mathbf{p}_2]dt &= \left(\frac{1}{T_0}\right)\int \mathbf{A}\cdot\left[\left(\frac{1}{a}\right)\boldsymbol{\nabla}a + i\boldsymbol{\nabla}\varphi\right]\mathbf{A}\cdot\mathbf{p}_2dt\\&\approx \left[\left(\frac{1}{a}\right)\partial_ja + i\partial_j\varphi\right]p_{2_i}\left(\frac{1}{T_0}\right)\int A_iA_jdt = \frac{1}{2}\left[\frac{1}{2}(\mathbf{p}_2\cdot\boldsymbol{\nabla}_Ta^2) + ia^2\mathbf{p}_2\cdot\boldsymbol{\nabla}_T\varphi\right]\;,\end{aligned} \tag{26}$$

where $\varphi \equiv k_0z - \omega_0t - \psi$. Thus the averaged value of the first term is

$$\left(\frac{1}{T_0}\right)\int \mathbf{p}_3\cdot\mathbf{A}^*dt = -\left(\frac{e}{mc\gamma_0\omega_0}\right)\left\{a^2\mathbf{p}_2\cdot\boldsymbol{\nabla}_T\psi + i\left[a^2\boldsymbol{\nabla}_T\cdot\mathbf{p}_2 + \frac{1}{2}\mathbf{p}_2\cdot\boldsymbol{\nabla}_Ta^2\right]\right\}\;, \tag{27}$$

where we have used the fact that $\nabla_T \varphi \equiv -\nabla_T \psi$. The averaged third order current can now be written as

$$\left(\frac{1}{T_0}\right) \int \mathbf{J}_3 \cdot \mathbf{A}^* dt \approx \left(\frac{e^2 n_0}{m\gamma_0 c}\right) \left\{ a^2 \left[\left(\frac{ea}{m\gamma_0 c}\right)^2 - 2\frac{\delta n_e}{n_0}\right] \right.$$

$$\left. + \left(\frac{1}{m\gamma_0 \omega_0}\right) \left[a^2 \, \mathbf{p}_2 \cdot \nabla_T \psi + i\left(a^2 \nabla_T \cdot \mathbf{p}_2 + \frac{1}{2}\mathbf{p}_2 \cdot \nabla_T a^2\right)\right] \right\}, \tag{28}$$

and the total current is given by

$$\left(\frac{1}{T_0}\right) \int \mathbf{J} \cdot \mathbf{A}^* dt \approx \left(\frac{e^2 n_0}{m\gamma_0 c}\right) \left\{ a^2 \left[\left(\frac{ea}{m\gamma_0 c}\right)^2 - 2N_e\right] \right.$$

$$\left. + \left(\frac{1}{m\gamma_0 \omega_0}\right) \left[a^2 \mathbf{p}_2 \cdot \nabla_T \psi + i\left(a^2 \nabla_T \cdot \mathbf{p}_2 + \frac{1}{2}\mathbf{p}_2 \cdot \nabla_T a^2\right)\right] \right\}, \tag{29}$$

where $N_e \equiv 1 + \frac{\delta n_e}{n_0}$. Using this expression we can now write the amplitude and phase equations from (7) & (8):

$$\frac{\partial^2}{\partial t^2} a = c^2 \nabla^2 a + a \left[\left(\frac{\partial \psi}{\partial t}\right)^2 - c^2 |\nabla \psi|^2\right] + 2a \left(\omega_0 \frac{\partial \psi}{\partial t} + ck_0 \frac{\partial \psi}{\partial z}\right)$$

$$+ \frac{1}{2}\left(\frac{\omega_p^2}{\gamma_0}\right) a \left[\left(\frac{ea}{m\gamma_0 c^2}\right)^2 - 2N_e + \left(\frac{1}{m\gamma_0 \omega_0}\right) \mathbf{p}_2 \cdot \nabla_T \psi\right] \tag{30}$$

and

$$\frac{\partial}{\partial t}\left(a^2 \frac{\partial \psi}{\partial t}\right) = c^2 \nabla \cdot (a^2 \nabla \psi) - 2a \left(\omega_0 \frac{\partial a}{\partial t} + ck_0 \frac{\partial a}{\partial z}\right)$$

$$- \frac{1}{2}\left(\frac{\omega_0}{\omega_p}\right)^2 \left(\frac{\omega_0}{m\gamma_0^2}\right) \left[a^2 \nabla_T \cdot \mathbf{p}_2 + \frac{1}{2}\mathbf{p}_2 \cdot \nabla_T a^2\right]. \tag{31}$$

The electrons are needed for calculating the electron density, N_e, appearing in the amplitude equation. When the equation of motion for electrons is averaged over the laser oscillation period, only two forces from the Lorentz force survive, the electrostatic force and the ponderomotive force, which are both second order in the quivering velocity:

$$\frac{d}{dt}\mathbf{p} = -e\mathbf{E}_s - mc^2 \nabla \sqrt{1 + \mu^2}. \tag{32}$$

10

Equations (30), (31) and (32) constitute the basic set of equations for our system in the slow time scale. As we remarked in the Introduction, they form the electromagnetic counterpart of the Zakharov equations in electrostatics. In the following we shall try to solve these basic equations.

III. Numerical Algorithm

From the form of the field equations one notices that the direction of the beam propagation singles out. Furthermore, the transverse directions appear only in terms involving inner products. This allows us to represent the transverse dimensions by one scalar variable (instead of a two dimensional vector), which we will call 'x'. The direction of beam propagation is labeled by 'y'. With these conventions the amplitude and phase equations are as follows:

$$\frac{\partial^2}{\partial t^2} a = c^2 \nabla^2 a + a \left[\left(\frac{\partial \psi}{\partial t} \right)^2 - c^2 |\nabla \psi|^2 \right] + 2\omega_0 a \left[\frac{\partial \psi}{\partial t} + c \frac{\partial \psi}{\partial y} \right]$$
$$+ \frac{1}{2} \left(\frac{\omega_p^2}{\gamma_0} \right) a \left[\left(\frac{ea}{m\gamma_0 c^2} \right) - 2N_e + \left(\frac{1}{m\gamma_0\omega_0} \right) p_{2x} \frac{\partial \psi}{\partial x} \right] \qquad (33)$$

and

$$\frac{\partial}{\partial t} \left(a^2 \frac{\partial \psi}{\partial t} \right) = c^2 (a^2 \nabla^2 \psi + \nabla a^2 \cdot \nabla \psi) - 2\omega_0 a \left(\frac{\partial a}{\partial t} + c \frac{\partial a}{\partial y} \right)$$
$$- \frac{1}{2} \left(\frac{\omega_0}{\omega_p} \right)^2 \left(\frac{\omega_0}{m\gamma_0^2} \right) \left[a^2 \frac{\partial p_{2x}}{\partial x} + \frac{1}{2} p_{2x} \frac{\partial a^2}{\partial x} \right] , \qquad (34)$$

where $\nabla \equiv \widehat{x} \frac{\partial}{\partial x} + \widehat{y} \frac{\partial}{\partial y}$.

The code solves for the four interdependent quantities, a, a_t, ψ, and ψ_t by the standard leap-frog integration over the four first order partial differential equations obtained from the above two equations. In addition the electrons are pushed and the electron density updated at every time step. The structure of the code is as follows:

11

- initialize fields

- initialize particles

- loop over the main program:

    - push particle positions

    - accumulate charge density and compute electrostatic field

    - update the amplitude and the time derivative of phase shift

    - calculate total force on particles and advance the grid momentum

    - update the phase shift and the time derivative of amplitude

    - update grid momentum and particle momentum

The boundary conditions are chosen to be periodic in both longitudinal (y) and transverse (x) directions. The width of the simulation system has to be chosen large enough compared to the width of the gaussian beam so that the parallel beams do not interact significantly with each other during the run.

The spatial differentiation may be performed using fast Fourier transforms to retain as high accuracy as possible. Unfortunately, the theoretical behavior of the phase shift, ψ, is such that at the edges in the transverse direction there is a discontinuity in the spatial derivative of ψ. This discontinuity is, of course, artificial, but fortunately it takes place in the region where it should have no significance (the amplitude, having a gaussian profile, has dropped to practically zero). However, when using Fourier transform, this effect will no longer be localized, but the sharp, unphysical structures will be instantaneously reflected all over the grid. Therefore we ended up adopting finite differencing for the spatial differentiation. This also eliminates the complex dealiasing technique[9] necessary with Fourier transforms to handle the equation $\frac{\partial \psi}{\partial t} = \frac{(a^2 \psi_t)}{a^2}$, which involves operation of the inverse.

Furthermore, it is important to notice that whenever the amplitude vanishes, the phase information is lost. This is reflected in the leap-frog equations in that the calculation for ψ_t involves division by a^2. To circumvent this problem that has arisen from our choice of independent variables (amplitude and phase instead of field components) and equations (wave equation instead of the set of Maxwell's equations), we introduce a ghost factor in evaluating the time derivative of the phase shift:

$$\psi_t = \frac{(a^2\psi_t)}{a^2} \rightarrow \frac{a^2(a^2\psi_t)}{a^4 + \epsilon^2} \; , \tag{35}$$

where ϵ^2 is a very small number (typically we have used $\epsilon^2 = (0.0001 \cdot a_0^2 - (0.001 \cdot a_0)^2)$. The ghost factor will have a negligible effect in the computation when the amplitude is finite, and it will prevent a divergence without altering the value of phase shift when the amplitude vanishes. We note that equation (35) is analytically continuously reducible to the original equation as $\epsilon^2 \rightarrow 0$.

IV. Testing of the Code: The Rayleigh Spread and Self-Focusing

The testing of the code was carried out by first excluding the plasma from the system by leaving out the plasma current terms in the field equations. This corresponds to electromagnetic beams propagating in vacuum. A beam with a gaussian intensity profile,

$$a = a_0 e^{-x^2/w_0^2} \; , \tag{36}$$

is considered. The evolution of a gaussian beam is reasonably well understood theoretically.[10] Assuming a stationary state, the behavior of the beam radius is given by the Rayleigh spreading,

$$w(y)^2 = w_0^2 \left[1 + \frac{y^2}{y_R^2} \right] \; , \tag{37}$$

13

where $y_R \equiv \frac{1}{2}k_0 w_0^2$ is the Rayleigh range. In the code, instead of assuming stationary state $\left(\frac{\partial}{\partial t} = 0\right)$, we give initially a beam uniform in y $\left(\frac{\partial}{\partial t} = 0\right)$. In doing this, the roles of time and direction of propagation get interchanged and we expect to see Rayleigh spreading in time rather than in space:

$$w(t)^2 = w_0^2 \left[1 + \frac{t^2}{T_R^2}\right] , \tag{38}$$

where T_R is the Rayleigh time corresponding to the Rayleigh range, $T_R \equiv \frac{1}{2}\omega_o \frac{w_0^2}{c^2}$. Instead of monitoring the beam radius, $w(t)$, we monitor the amplitude, noting that the total power is invariant:

$$P_3 \equiv a_0^2 w_0^2 = a(t)^2 w(t) \qquad \text{in 3 dimensions}$$

$$P_2 \equiv a_0^2 w_0 = a(t)^2 w(t) \qquad \text{in 2 dimensions .}$$

The behavior of the peak amplitude is thus specified by the behavior of the beam radius, and so we can equally well follow the evolution of the amplitude. In Fig. 1(a) we have plotted the time behavior of the peak amplitude obtained from the simulation run, together with the theoretical curve. The two curves are identical until after about three Rayleigh times they start diverging. This is due to the significant overlapping at the skirts of the beam we are monitoring with the identical beams parallel to it (see Fig. 1(b)) that exist outside the simulation box due to the choice of periodic boundary conditions.

To further test the field solver, we include the plasma effects — not in a particle description but in terms of the field quantities via theoretical formulae. First, consider the case in which the self-focusing is solely due to the relativistic mass increase of the electrons.[11] The dispersion relation for electromagnetic waves in vacuum, $\omega_0 = ck_0$, is then replaced by the plasma dispersion relation, $\omega_0 = \sqrt{\omega_p^2 + c^2 k_0^2}$, for the zeroth order solution in the amplitude equation, and a term quadratic in amplitude is added into the field equations. According to Ref. 11 at low intensities the beam should diffract, but above a critical intensity we should see self-focusing. The value estimated for the critical intensity is (in three dimensions)

$$I_{\text{cr}} \approx \left(\frac{\lambda_c}{w_0}\right)^2 , \tag{39}$$

14

where λ_c is the collisionless skin depth and the intensity is defined as the normalized quivering velocity of the laser,

$$I \equiv \frac{e^2 E^2}{m^2 \omega_0^2 c^2} . \qquad (40)$$

We ran the code with parameters $\lambda_c = 0.9 \frac{c}{\omega_p}$, $w_0 = 4.0 \frac{c}{\omega_p}$ and saw self-focusing take over the diffraction at intensities higher than $I \sim 0.05$, whereas the prediction for critical intensity (for two dimensional case) given by Schmidt and Horton is $I_{cr} = 0.07$ for these parameters. The agreement seems reasonably good.

Next we included self-focusing terms due to the ponderomotive force. This was done by assuming that the system had reached a state in which the ponderomotive force acting on electrons is balanced by the electrostatic force due to the charge separation (induced by the ponderomotive force).[12] In this model the electron density is given by (in two spatial dimensions)

$$N_e \equiv \frac{n_e}{n_0} = \left(\frac{c}{\omega_p} \right)^2 \frac{\partial}{\partial x} \sqrt{1 + \left(\frac{eE}{m\omega_0 c^2} \right)^2} . \qquad (41)$$

The theoretical prediction for the critical intensity in this case is (for two dimensions)

$$I_{cr} \approx \frac{1}{\sqrt{2}} \frac{\lambda_c}{w_0} . \qquad (42)$$

For the parameters given above the self-focusing threshold is still given by $I_{cr} = 0.07$, whereas our simulation yielded $I_{cr} \approx 0.05$. It should be noticed that the time scale for self-focusing of ponderomotive origin is much longer than that for relativistic self-focusing. This is because in the ponderomotive self-focusing a net flux of electrons has to move appreciable distances, whereas the relativistic effect is almost instantaneous. This is the reason why the critical intensity for the onset of the self-focusing was dominated by the relativistic effects even when the ponderomotive effects were included.

As the next stage of testing, we included dynamical electrons and stationary ions in the system. The electrons are pushed at every time step using ponderomotive and electrostatic forces, and from their positions the plasma density and electrostatic forces can be derived.

15

One dimensional test has been carried out (the direction of propagation is taken to be uniform, thus modeling an infinite beam). In Fig. 2(a) few time histories from these runs are shown. We have used 100 particles per grid cell. The width of the simulation system is $25.6 \frac{c}{\omega_p}$, the frequency of the laser is $5\omega_p$ and the radius of the beam is $w_0 = 4.0 \frac{c}{\omega_p}$. The thermal velocity of the electrons is one tenth of the speed of light thus corresponding to a 5 keV plasma. At low intensities the beam diffracts as indicated by the reducing amplitude for $I_0 = 0.15$ (Fig. 2a) and at higher intensities, like $I_0 = 0.36$, we see an increase in amplitude implicating self-focusing (Fig. 2b). The critical intensity given by the theoretical model is $I_{cr} = 0.18$ for these parameters, whereas in the simulations it was observed to be approximately $I_{cr} \sim 0.20$.

V. Conclusions

We have presented a new kind of a particle simulation algorithm intended for studying the long time scale evolution or transport of an electromagnetic beam in plasma. In particular, we have used it to study self-focusing of a laser beam in plasma.

The code is based on a set of equations consisting of the wave equation written in terms of the vector and scalar potentials, and the equation of motion the particles averaged over the rapid laser oscillations. This way the code does not need to resolve for the rapid oscillations and the modulation can be seen directly as the primary evolution of the beam.

For the intended application[12] the ions were assumed to be stationary and only electrons were being advanced. Even in this simplified form the test runs of the code gave results that are in agreement with the theoretical work done in the field of self-focusing in plasma.

When implementing the two dimensional version of the code (by including dynamics in the direction of propagation) we also move the simulation system into a frame moving at the group velocity of the laser beam. This way we can follow the beam far in the direction of propagation without great computational costs (that would be brought about when following

16

the beam in laboratory frame by including an extensive grid).

Acknowledgments

References

1. T. Tajima and J.M. Dawson, Phys. Rev. Lett. **43**, 267 (1979).

2. T. Tajima, *Laser and Particle Beams* vol. 3 part 4, 351 (1985).

3. C. Joshi et al., Nature (London) **311**, 525 (1984).

4. For example, W. Horton and T. Tajima, Phys. Rev. **A34**, 4110 (1986).

5. T. Tajima in *Proc. 12th International Conference on High Energy Accelerators*, eds. F.T. Cole and R. Donaldson (Fermi National Accelerator Laboratory, Batavia, Illinois 1983) p. 470.

6. V.E. Zakharov, Zh. Exp. Teor. Fiz. **62**, 1745 (1972) [Sov. Phys. JETP **35**, 908 (1972)].

7. L.M. Degtyarev, I.M. Ibragimov, R.Z. Sagdeev, G.I. Solov'ev, V.D. Shapiro, and V.I. Shevchenko, Pis'ma Zh. Eksp. Theor. Fiz. **40**, 455 (1984) [JETP Lett. **40**, 1282 (1984)].

8. D. Russell, D.F. Dubois, and H.A. Rose, Phys. Rev. Lett. **60**, 581 (1988).

9. T. Tajima, *Computational Plasma Physics*, Chap. 6, to be published by Addison-Wesley (Reading, Massachusetts 1988).

10. e.g. W. Demtroder, *Laser Spectroscopy* (Springer-Verlag, Berlin 1982).

11. G. Schmidt and W. Horton, Comm. Plasma Phys. Controlled Fusion E, 9, 85 (1985).

12. D.C. Barnes, T. Kurki-Suonio, and T. Tajima, IEEE Transactions on Plasma Science, PS-15, 154 (1987).

Figure Captions

Figure 1. Rayleigh spread of a laser beam.

(a) The ratio of the instantaneous amplitude (at the beam axis) to the initial one is plotted as given by the simulation code. For comparison, also the curve given by the two dimensional diffraction theory is included.

(b) Radial profile of a gaussian beam at different times as given by the diffraction theory. After about three Rayeigh spreading times the beam is seen to extend significantly outside the simulation box and thus it will, due to the periodic conditions, cause noticeable interference effects.

Figure 2. Evolution of a gaussian beam propagating in plasmas as given by the simulation code using full electron dynamics.

(a) $I < I_{cr}$: The beam diffracts.

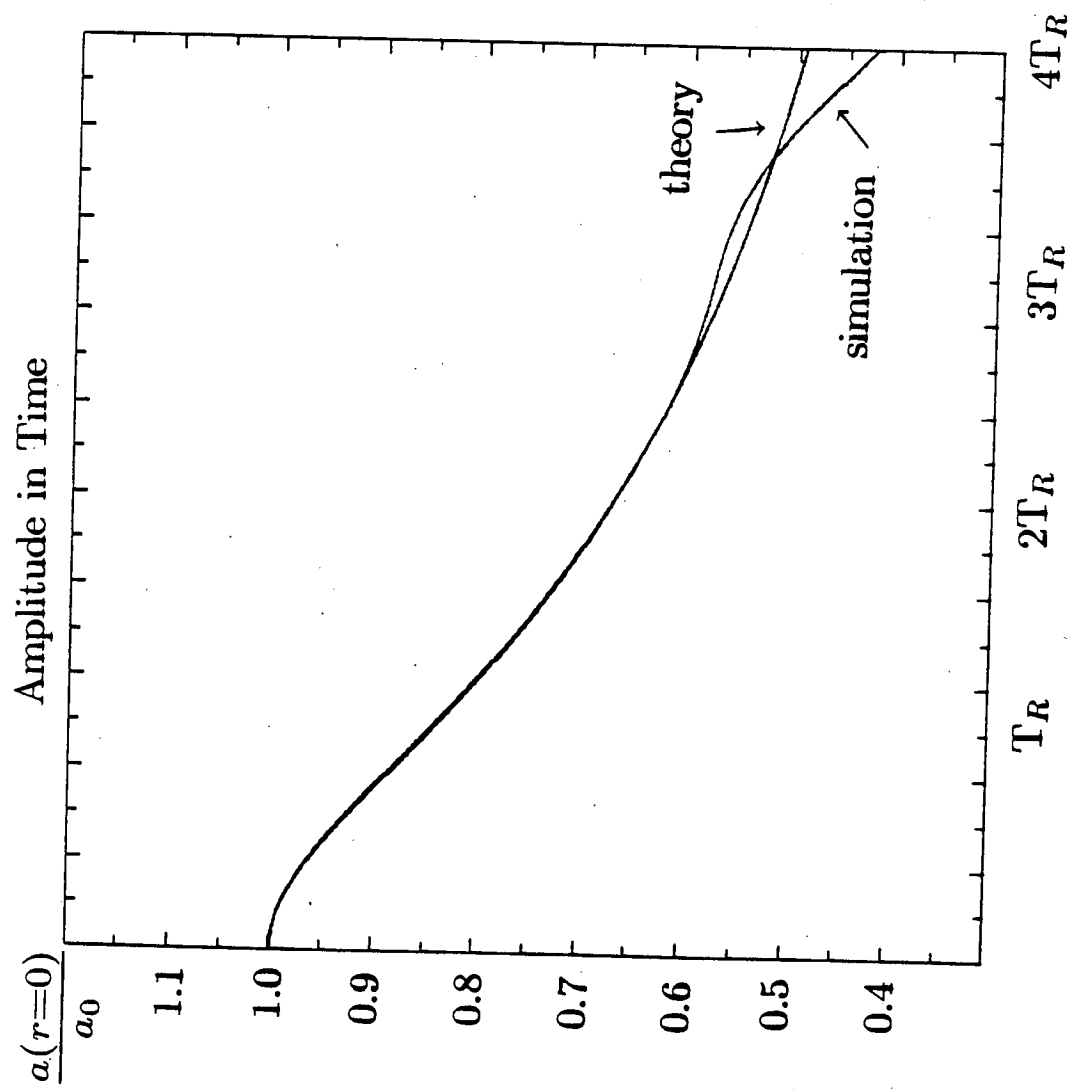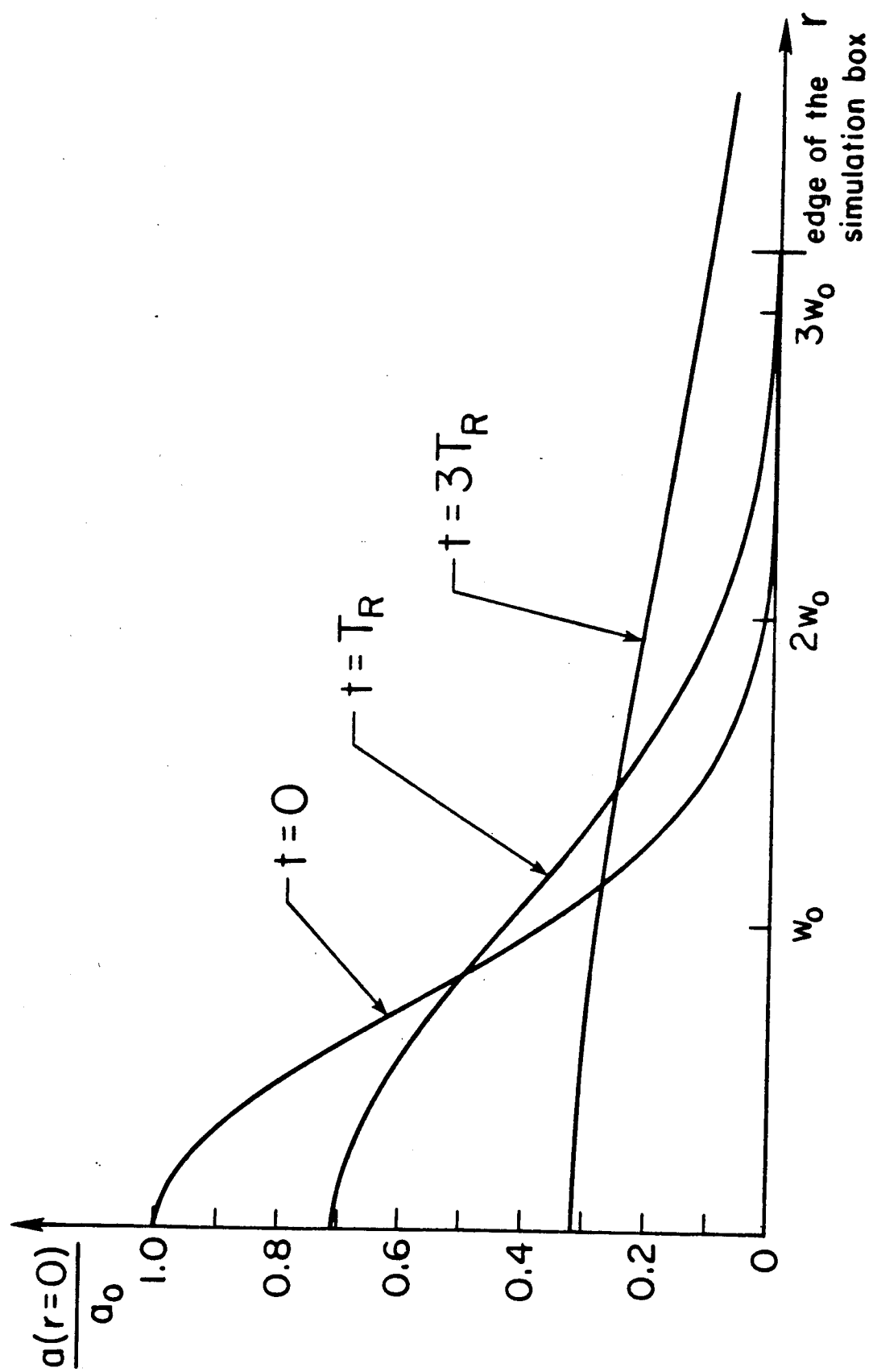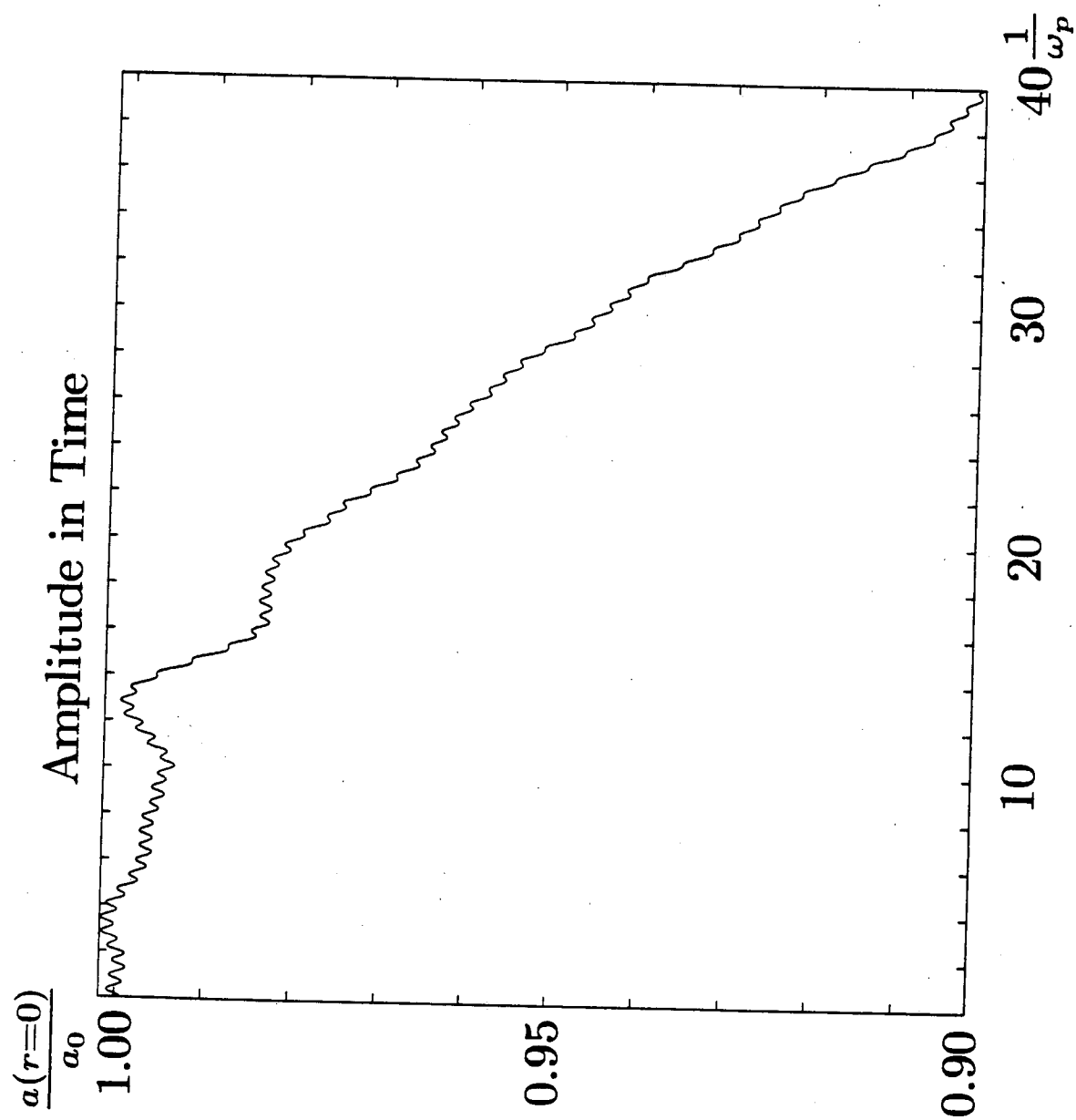(b) $I > I_{cr}$: The beam is self-focused followed by diffraction.

Amplitude in Time

$\dfrac{a(r=0)}{a_0}$

theory

simulation

T_R $2T_R$ $3T_R$ $4T_R$

Figure 1a

Figure 1b

Amplitude in Time

$\dfrac{a(r=0)}{a_o}$

Figure 2a

Amplitude in Time

$\dfrac{a(r=0)}{a_0}$

Figure 2b